

# Coordination of Dimethyl Methylphosphonate to the Bidentate Lewis Acid 1,2-Bis(chloromercurio)tetrafluorobenzene

Martin Tschinkl,<sup>†</sup> Robert E. Bachman,<sup>‡</sup> and François P. Gabbaï<sup>\*,†</sup>

Departments of Chemistry, Texas A&M University, College Station, Texas 77843-3255, and Georgetown University, Washington, DC 20057

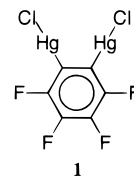
Received December 13, 1999

**Summary:** Incremental addition of the nerve gas simulant dimethyl methylphosphonate (DMMP) to an acetone solution of the bidentate Lewis acid 1,2-bis(chloromercurio)tetrafluorobenzene results in a downfield shift of the <sup>199</sup>Hg NMR resonance. This phenomenon is explained by the formation of a complex involving the bifunctional Lewis acid and DMMP with a stability of 3.7 (±0.4) M<sup>-1</sup>. Upon cooling of a hot solution of 1,2-bis(chloromercurio)tetrafluorobenzene in neat DMMP, needlelike crystals of a 1:2 complex are formed. This compound has been characterized by IR, <sup>31</sup>P{<sup>1</sup>H} CP/MAS NMR, elemental analysis, and X-ray single-crystal analysis. The structural data show that the phosphoryl oxygen atom of each DMMP bridges the two mercury centers of the bidentate Lewis acid. The individual adduct molecules interact by intermolecular Hg...Cl contacts, which leads to the formation of polymeric chains. Each chain interacts with two neighboring chains via formation of offset π-π contacts. These weak interactions result in the formation of layers that sandwich the coordinated DMMP molecules.

been demonstrated that bidentate Lewis acids form complexes with organic carbonyls in which the carbonyl oxygen atom undergoes concomitant coordination to the two Lewis acidic centers.<sup>4–6</sup> The formation of such adducts has been advanced to rationalize the unusual activity of bifunctional Lewis acid catalysts.<sup>10,11</sup> In principle, bidentate Lewis acids could serve as receptors for other substrates containing terminal oxo functionalities. Available examples that do not involve organic carbonyls are scarce and are limited to sulfoxides.<sup>12–14</sup> Taking into account the ubiquity of organophosphorus(V) esters in chemical warfare agents,<sup>15</sup> we have decided to determine whether bidentate Lewis acids could coordinate phosphonate esters. As part of our ongoing investigation into the coordination chemistry of 1,2-bis(chloromercurio)tetrafluorobenzene (**1**),<sup>5,13</sup> we now wish to report our findings on the interaction of **1** with dimethyl methylphosphonate (DMMP), a substrate sometimes used as nerve gas simulant.<sup>16</sup>

## Introduction

Polydentate Lewis acids have emerged as useful receptors for anionic and neutral basic substrates.<sup>1–9</sup> While great emphasis has been placed on the recognition of anionic guests,<sup>1–3</sup> only a few studies have focused on the binding of neutral molecules.<sup>4–9</sup> However, it has



**1**

<sup>†</sup> Texas A&M University.

<sup>‡</sup> Georgetown University.

- (1) (a) Schmidtchen, F. P.; Berger, M. *Chem. Rev.* **1997**, *97*, 1609–1646. (b) Dietrich, B. *Pure Appl. Chem.* **1993**, *65*, 1457–1464. (c) Kaufmann, D. E.; Otten, A. *Angew. Chem., Int. Ed. Engl.* **1994**, *33*, 1832–1834.
- (2) (a) Hawthorne, M. F.; Zheng, Z. *Acc. Chem. Res.* **1997**, *30*, 267–276. (b) Hawthorne, M. F. *Pure Appl. Chem.* **1994**, *66*, 245–254.
- (3) (a) Uhl, W.; Hannemann, F. J. *Organomet. Chem.* **1999**, *579*, 18–23. (b) Williams, V. C.; Piers, W. E.; Clegg, W.; Elsegood, M. R. J.; Collins, S.; Marder, T. B. *J. Am. Chem. Soc.* **1999**, *121*, 3244–3245. (c) Altmann, R.; Jurkschat, K.; Schurmann, M.; Dakternieks, D.; Duthie, A. *Organometallics* **1998**, *17*, 5858–5866. (d) Tschinkl, M.; Schier, A.; Riede, J.; Gabbaï, F. P. *Inorg. Chem.* **1997**, *36*, 5706–5711. (e) Tikhonova, I. A.; Dolgushin, F. M.; Yanovsky, A. I.; Struchkov, Yu. T.; Gavrilova, A. N.; Saifkulova, L. N.; Shubina, E. S.; Epstein, L. M.; Furin, G. G.; Shur, V. B. *J. Organomet. Chem.* **1996**, *508*, 271–273. (f) Newcomb, M.; Horner, J. H.; Blanda, M. T.; Squattrito, P. J. *J. Am. Chem. Soc.* **1989**, *111*, 6294–6301. (g) Wuest, J. D.; Zacharie, B. *Organometallics* **1985**, *4*, 410–411. (h) Katz, H. E. *J. Org. Chem.* **1985**, *50*, 5027–5032.
- (4) (a) Wuest, J. D. *Acc. Chem. Res.* **1999**, *32*, 81–89. (b) Simard, M.; Vaugois, J.; Wuest, J. D. *J. Am. Chem. Soc.* **1998**, *120*, 13016–13022. (c) Vaugois, J.; Simard, M.; Wuest, J. D. *Coord. Chem. Rev.* **1995**, *95*, 55–73.
- (5) Tschinkl, M.; Schier, A.; Riede, J.; Gabbaï, F. P. *Organometallics* **1999**, *18*, 1747–1753.
- (6) Reilly, M.; Oh, T. *Tetrahedron Lett.* **1995**, *36*, 217–220.

- (7) (a) Saied, O.; Simard, M.; Wuest, J. D. *Organometallics* **1998**, *17*, 1128–1133. (b) Gabbaï, F. P.; Schier, A.; Riede, J.; Hynes, M. J. *J. Chem. Soc., Chem. Commun.* **1998**, 897–898. (c) Nozaki, K.; Yoshida, M.; Takaya, H. *Bull. Chem. Soc. Jpn.* **1996**, *69*, 2043–2052. (d) Katz, H. E. *J. Org. Chem.* **1989**, *54*, 2179–2183.
- (8) (a) Wuest, J. D.; Zacharie, B. *J. Am. Chem. Soc.* **1987**, *109*, 4714–4715. (b) Nadeau, F.; Simard, M.; Wuest, J. D. *Organometallics* **1990**, *9*, 1311–1314.
- (9) (a) Zinn, A. A.; Zheng, Z.; Knobler, C. B.; Hawthorne, M. F. *J. Am. Chem. Soc.* **1996**, *118*, 70–74. (b) Yang, X.; Knobler, C. B.; Zheng, Z.; Hawthorne, M. F. *J. Am. Chem. Soc.* **1994**, *116*, 7142–7159.
- (10) (a) Ooi, T.; Tomoya, M.; Maruoka, K. *Angew. Chem., Int. Ed.* **1998**, *37*, 2347–2349. (b) Ooi, T.; Takahashi, M.; Maruoka, K. *J. Am. Chem. Soc.* **1996**, *118*, 11307–11308.
- (11) For the activation of conjugated thioketones, see: Lee, H.; Diaz, M.; Hawthorne, M. F. *Tetrahedron Lett.* **1999**, *40*, 7651–7655.
- (12) Schmidbaur, H.; Öller, H.-J.; Wilkinson, D. L.; Huber, B. *Chem. Ber.* **1989**, *122*, 31–36.
- (13) Tschinkl, M.; Schier, A.; Riede, J.; Gabbaï, F. P. *Angew. Chem., Int. Ed.* **1999**, *38*, 3547–3549.
- (14) Karol, T. J.; Hutchinson, J. P.; Hyde, J. R.; Kuivila, H. G.; Zubietta, J. A. *Organometallics* **1983**, *2*, 106–114.
- (15) (a) Yang, Y.-C.; Baker, J. A.; Ward, J. R. *Chem. Rev.* **1992**, *92*, 1729–1743. (b) Yang, Y.-C. *Acc. Chem. Res.* **1999**, *32*, 109–115.
- (16) (a) Segal, S. R.; Suib, S. L.; Satyapal, S.; Tang, X.; Washmon, L. *Book of Abstracts*, 217th National Meeting of the American Chemical Society, Anaheim, CA, March 21–25, 1999; American Chemical Society: Washington, DC, 1999. (b) Taranenko, N.; Alarie, J.-P.; Stokes, D. L.; Vo-Dinh, T. *J. Raman Spectrosc.* **1996**, *27*, 379–384. (c) Nieuwenhuizen, M. S.; Hartevel, J. L. N. *Talanta* **1994**, *41*, 461–472.

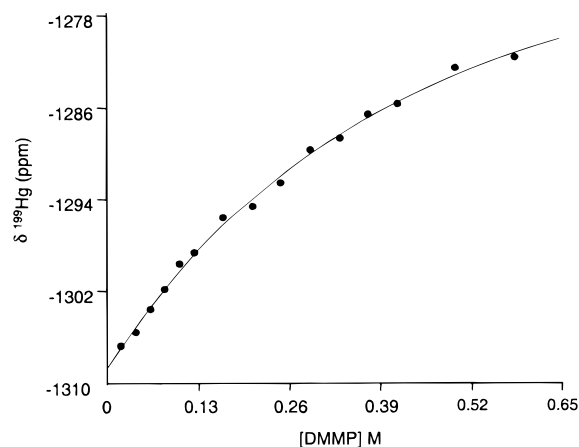


**Figure 1.**  $^{199}\text{Hg}$  chemical shift of **1** in acetone vs concentration of DMMP.  $[\mathbf{1}] = 0.187\text{ M}$ .

## Results and Discussion

**Solution Studies.** Upon incremental addition of DMMP to a solution of **1** in acetone, the  $^{199}\text{Hg}$  NMR resonance of **1** undergoes a downfield shift (Figure 1). It has been previously demonstrated that the  $^{199}\text{Hg}$  NMR resonance of organomercurials undergoes an upfield shift when the polarity of the solvent is increased.<sup>17</sup> Therefore, it is likely that the downfield shift observed upon addition of DMMP to a solution of **1** reflects the formation of a complex involving **1** and DMMP. The curve was fitted with a model based on a 1:1 complex. From this model, a stability constant of  $3.7 (\pm 0.4)\text{ M}^{-1}$  was obtained. Attempts to fit the curve on the basis of other models were unsuccessful, suggesting that the 1:1 complex **1**-DMMP (**2**) is the main species formed in solution. The magnitude of the stability constant is rather small and reflects the noninnocent role of acetone, which forms a 1:1 complex with **1**.<sup>5</sup> The stability constant determined for DMMP falls between those determined for DMSO ( $8\text{ M}^{-1}$ ) and DMF ( $1.8\text{ M}^{-1}$ ), which allows the following selectivity order to be established for **1**: DMSO > DMMP > DMF > acetone.<sup>5</sup>

**Solid-State Studies.** In an effort to isolate a complex involving **1** and DMMP, **1** was dissolved in neat hot DMMP. Upon cooling of the resulting solution, needle-like crystals of a new complex (**3**) formed. Elemental analysis data indicated that the composition of **3** corresponds to that of the 1:2 complex **1**-(DMMP)<sub>2</sub>. The  $^{31}\text{P}\{-^1\text{H}\}$  CP/MAS NMR spectrum of **3** exhibits two slightly deshielded resonances at 35.6 and 37.5 ppm<sup>18</sup> which indicates the presence of two nonequivalent DMMP molecules (Figure 2). It is noteworthy that the resonance at 37.5 ppm is broad and probably corresponds to the DMMP molecule affected by positional disorder (vide infra). The IR spectrum of **3** features a broad unresolved absorption at  $1234\text{ cm}^{-1}$  assigned to  $\nu_{\text{P=O}}$ . Comparison with the stretching frequency of neat DMMP ( $\nu_{\text{P=O}} = 1243\text{ cm}^{-1}$ ) indicates a moderate weakening of the P=O bond.

The crystal structure of **3** has been determined by X-ray diffraction analysis. Pertinent crystallographic

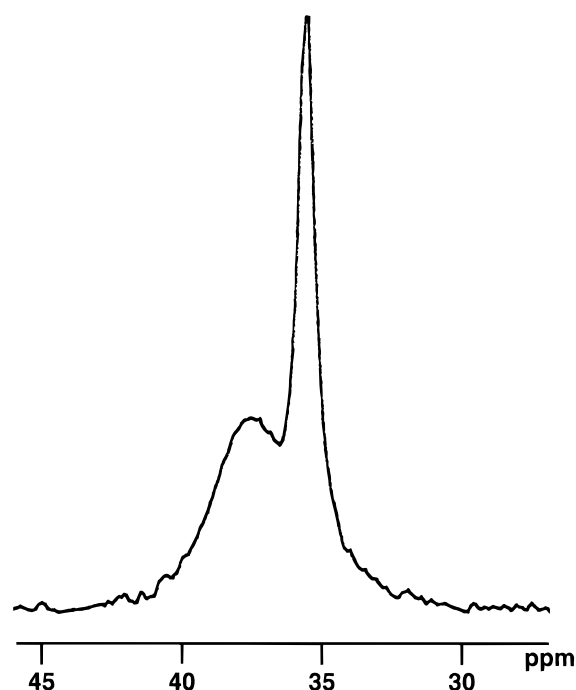


**Figure 2.**  $^{31}\text{P}\{-^1\text{H}\}$  CP/MAS NMR spectrum of **3**.

**Table 1. Crystal Data and Structure Refinement Details for **3****

empirical formula	$\text{C}_{12}\text{H}_{18}\text{Cl}_2\text{F}_4\text{Hg}_2\text{O}_6\text{P}_2$
fw	868.28
temp	173 K
wavelength	0.710 73 Å
cryst syst	monoclinic
space group	$P2_1/c$ (No. 14)
unit cell dimens	
<i>a</i>	11.3157(11) Å
<i>b</i>	14.5575(14) Å
<i>c</i>	14.3683(14) Å
$\alpha$	90°
$\beta$	108.110(2)°
$\gamma$	90°
<i>V</i>	2249.6(4) Å <sup>3</sup>
<i>Z</i>	4
density (calcd)	2.564 g/cm <sup>3</sup>
abs coeff	14.069 mm <sup>-1</sup>
<i>F</i> (000)	1592
cryst size	0.40 × 0.06 × 0.02 mm <sup>3</sup>
$\theta$ range for data collec	1.89–28.34°
index ranges	$-15 \leq h \leq 14$ , $-19 \leq k \leq 19$ , $-19 \leq l \leq 19$
no. of rflns collected	18 914
no. of indep rflns	5476 ( $R(\text{int}) = 0.0584$ )
completeness to $\theta = 28.34^\circ$	97.5%
abs cor	SADABS
max, min transmissn	0.7661, 0.0708
refinement method	full-matrix least squares on $F^2$
no. of data/restraints/params	5476/7/258
goodness of fit on $F^2$	0.948
final <i>R</i> indices ( $I > 2\sigma(I)$ )	$R1 = 0.0324$ , $wR2 = 0.0614$
<i>R</i> indices (all data)	$R1 = 0.0630$ , $wR2 = 0.0671$
extinction coeff	0.000 24(4)
largest diff peak and hole	1.660 and $-1.071\text{ e Å}^{-3}$

data are assembled in Table 1. The asymmetric unit of **3** consists of one molecule of **1**( $\mu_2$ -DMMP)<sub>2</sub> (Figure 3). Each of the coordinated DMMP molecules is chelated by the bidentate Lewis acidic pincer, and the resulting Hg–O bonds are approximately perpendicular to the respective C–Hg–Cl sequences. The Hg–O bond distances (average 2.79 Å) are shorter than the sum of the van der Waals radii of oxygen (1.54 Å)<sup>19</sup> and mercury

(17) (a) Sens, M. A.; Wilson, N. K.; Ellis, P. D.; Odom, J. D. *J. Magn. Reson.* **1975**, *19*, 323–336. (b) Kidd, R. G.; Goodfellow, R. J. In *NMR and the Periodic Table*; Harris, R. K., Mann, B. E., Eds.; Academic Press: London, 1978; pp 195–278.

(18) For comparison, DMMP in  $\text{CDCl}_3$  gives rise to a resonance at 33.5 ppm.

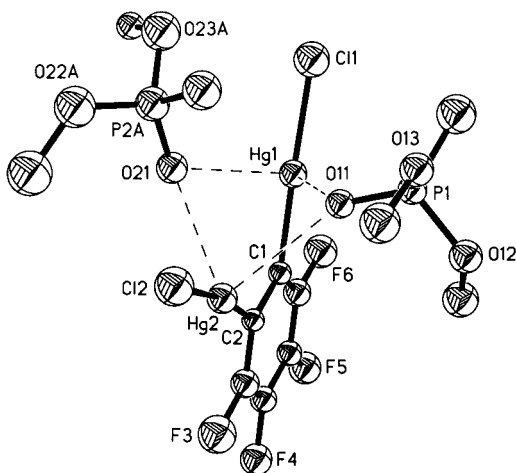


**Figure 3.** ORTEP diagram of **3** (50% thermal ellipsoids). For clarity reasons, only one conformation of the disordered DMMP molecule is shown. Selected bond lengths (Å) and angles (deg): Hg(1)–C(1) = 2.064(7), Hg(1)–Cl(1) = 2.3110(17), Hg(2)–C(2) = 2.068(6), Hg(2)–Cl(2) = 2.3175(17), P(1)–O(11) = 1.467(5), P(1)–O(13) = 1.563(5), P(1)–O(12) = 1.570(5), O(21)–P(2B) = 1.461(7), O(21)–P(2A) = 1.515(6), P(2A)–O(22A) = 1.524(14), P(2A)–O(23A) = 1.545(12), P(2A)–C(21A) = 1.786(15), P(2B)–O(22B) = 1.461(12), P(2B)–O(23B) = 1.618(11); C(1)–Hg(1)–Cl(1) = 171.49(18), C(2)–Hg(2)–Cl(2) = 172.26(18). Selected intermolecular bond distances (Å) and angles (deg): Hg(1)–O(11) = 2.722, Hg(1)–O(21) = 2.760, Hg(2)–O(11) = 2.832, Hg(2)–O(21) = 2.849; C(1)–Hg(1)–O(11) = 89.7, Cl(1)–Hg(1)–O(11) = 97.6, C(1)–Hg(1)–O(21) = 91.2, Cl(1)–Hg(1)–O(21) = 94.6, O(11)–Hg(1)–O(21) = 78.1, C(2)–Hg(2)–O(11) = 88.6, Cl(2)–Hg(2)–O(11) = 98.6, C(2)–Hg(2)–O(21) = 89.5, Cl(2)–Hg(2)–O(21) = 95.1, O(11)–Hg(1)–O(21) = 74.9.

(1.73–2.00 Å).<sup>20</sup> They are, however, longer than those measured in **1**·( $\mu_2$ -acetone) (average 2.73 Å),<sup>5</sup> **1**·( $\mu_2$ -DMF)<sup>5</sup> (average 2.70 Å), and **1**·( $\mu_2$ -DMSO)<sub>2</sub><sup>13</sup> (average 2.70 Å), which substantiates the presence of a rather weak interaction. The coordination geometry at O(11) slightly deviates from a trigonal-planar arrangement (sum of the bond angles of 356.3°). Part of the DMMP molecule at O(21) is disordered (see Experimental Section). As a result of this disorder, two types of coordination geometries are observed for O(21), which shows an increased pyramidality when compared to O(11) (sums of the bond angles at O(21) are equal to 351.4 and 324.9° for P(2B) and P(2A), respectively). While the P=O bond distances in the disordered phosphonate molecule could not be determined with accuracy, the P(1)–O(11) bond (1.467(5) Å) does not appear to be lengthened when compared to the range of 1.448–1.470 Å obtained for several compounds featuring a noncoordinated dimethylphosphonate moiety.<sup>21</sup> This observation contrasts with the IR and <sup>31</sup>P NMR

(19) Nyburg, S. C.; Faerman, C. H. *Acta Crystallogr., Sect. B* **1985**, *41*, 274–279.

(20) Canty, A. J.; Deacon, G. B. *Inorg. Chim. Acta* **1980**, *45*, L225–L227.

(21) (a) Baudy, R. B.; Greenblatt, L. P.; Jirkovsky, I. L.; Conklin, M.; Russo, R. J.; Bramlett, D. R.; Emrey, T. A.; Simmonds, J. T.; Kowal, D. M.; Stein, R. P.; Tasse, R. P. *J. Med. Chem.* **1993**, *36*, 331–42. (b) Mikolajczyk, M.; Mikina, M.; Wiczorek, M. W.; Blaszczyk, J. *Angew. Chem., Int. Ed. Engl.* **1996**, *35*, 1560–1562. (c) Bourne, S.; Modro, A. M.; Modro, T. A. *Phosphorus, Sulfur Silicon Relat. Elem.* **1995**, *102*, 83–90. (d) Watson, W. H.; Nagl, A.; Marchand, A. P.; Reddy, G. M.; Reddy, S. P.; Dave, P. R. *Acta Crystallogr., Sect. C: Cryst. Struct. Commun.* **1989**, *C45*, 263–267.

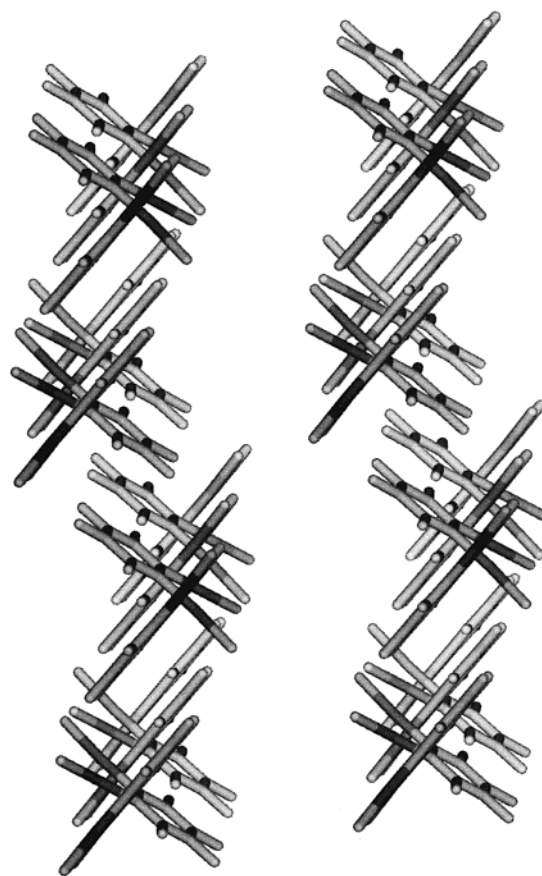


**Figure 4.** View showing the perpendicular arrangement of the monomers in each chain. The formation of  $\pi$ – $\pi$  contacts and layers is also obvious from this view.

**Table 2.** Intermolecular Hg···Cl and Hg···Hg and C···C Distances (Å) in the Supramolecular Structure of **3**

Hg(1)–Cl(2) <sup>a</sup>	3.662	Hg(1)–Hg(2) <sup>a</sup>	3.778
Hg(1)–Cl(2) <sup>b</sup>	3.311	C(4)–C(5) <sup>c</sup>	3.529

<sup>a</sup>  $x, 0.5 - y, 0.5 + z$ . <sup>b</sup>  $x, 0.5 - y, -0.5 + z$ . <sup>c</sup>  $-x + 1, -y, -z + 2$ .

spectroscopic data, which suggest a polarization of the P=O bond. A similar situation is encountered in analogous ketone and formamide complexes.<sup>4,5</sup> In these complexes, while a significant lengthening of the C=O bond is hard to confirm, the double coordination of the carbonyl functionality has been shown to have measurable effects on the spectroscopic<sup>4,5</sup> and chemical properties<sup>4b</sup> of the bound carbonyl substrate.

Examination of the cell-packing diagram reveals the existence of infinite parallel polymeric chains in which the successive molecules of **1** form a dihedral angle of 87.7° and are therefore essentially perpendicular (Figure 4). Thus, while organomercury halides usually polymerize through the formation of flat Hg<sub>2</sub>Cl<sub>2</sub> bridges,<sup>22</sup> the orientation of the successive molecules in **3** leads to the formation of a distorted Hg<sub>2</sub>Cl<sub>2</sub> tetrahedron as a bridging unit. The Hg···Cl contacts are smaller than the sum of the van der Waals radii ( $r_{vdW}(\text{Cl}) = 1.58$ – $1.78$  Å,<sup>19</sup>  $r_{vdW}(\text{Hg}) = 1.73$ – $2.00$  Å)<sup>20</sup> (Table 2). Interestingly, this arrangement leads to the formation of a relatively short Hg···Hg distance (3.778 Å) which is only slightly longer than the mercuriphilic contacts of 3.455–3.673

(22) Tschinkl, M.; Schier, A.; Riede, J.; Gabbai, F. P. *Organometallics* **1998**, *17*, 2921–2923. Tschinkl, M.; Schier, A.; Riede, J.; Gabbai, F. P. *Organometallics* **1999**, *18*, 2040–2042.



Å observed in the structure of tris(1,3-dimethyluracil-5-yl)mercuriooxonium salts (Table 2).<sup>23</sup> Each chain interacts with two neighboring chains via formation of offset  $\pi$ - $\pi$  contacts of 3.52 Å.<sup>24</sup> In this offset arrangement, the shortest inter-ring contact occurs between the C(4) and the C(5) carbon atoms of juxtaposed rings (Table 2). As a result of this interaction, the successive chains form parallel layers that sandwich the coordinated DMMP molecules.

### Conclusion

This work demonstrates that simple bidentate Lewis acids such as **1** can be used to complex phosphonate esters. Both solution and solid-state studies indicate the presence of a rather weak interaction between **1** and DMMP. The low affinity of mercury for hard oxygen donors and the steric bulk of DMMP likely account for this situation. Nevertheless, the crystal structure of **3** establishes that the phosphoryl oxygen atom of DMMP is concomitantly ligated to the two metal centers. We note finally that a similar double coordination of the phosphoryl oxygen atom is sometimes encountered in the binding of organophosphorus(V) substrates at the active site of dinuclear metalloenzymes involved in phosphate metabolism.<sup>25</sup>

### Experimental Section

**General Considerations.** <sup>199</sup>Hg NMR (35.7 MHz) were recorded on a Varian XL 200 broadband spectrometer at 25 °C with HgMe<sub>2</sub> as an external standard. The solid-state <sup>31</sup>P-{<sup>1</sup>H} CP/MAS NMR spectra were recorded on a Bruker MSL 300 spectrometer operating at a field strength of 7.05 T. Cross-polarization and high-power proton decoupling were applied with a 90° pulse time of 4 μs, a contact time of 1 ms, and a recycle delay of 5 s. Alternatively, direct excitation with a 45° pulse and high-power proton decoupling were applied with a recycle delay of 60 s. <sup>31</sup>P NMR shifts are referenced to an external sample of phosphoric acid, with the signal set to 0 ppm. Approximately 50 mg of sample was packed into a 7 mm ZrO<sub>2</sub> Bruker rotor with Kel-F inserts and cap. The rotor spinning speed was 4.8 kHz. All NMR measurements were acquired at ambient temperature. Atlantic Microlab (Norcross, GA) performed the elemental analyses. The infrared spectra were recorded as KBr pellets on a Mattson Genesis Series FTIR. All melting points were measured on samples in sealed capillaries and are uncorrected. All solvents were distilled before use and stored over molecular sieves. Compound **1** was prepared by following the published procedure.<sup>26</sup> Dimethyl methylphosphonate was purchased from Aldrich and used as provided.

**<sup>199</sup>Hg NMR Titration Experiment.** The titration curve depicted in Figure 1 was obtained by incremental addition of small amounts of the DMMP to an acetone-*d*<sub>6</sub> solution (0.7 mL) of **1** (81 mg, 0.131 mmol). A 25 μL syringe was used to add DMMP directly into the NMR tube containing the solution of **1**. After each addition the <sup>199</sup>Hg NMR chemical shift of the sample was measured. The program EQNMR was used to

calculate the stability constant *K*.<sup>27</sup> The data were not corrected for the slight change in volume produced by the addition of titrant. *K* is defined as  $K = [\mathbf{1} \cdot \text{DMMP}] / ([\mathbf{1}][\text{DMMP}])$ . The approximation that  $[\mathbf{1}] = [\mathbf{1} \cdot \text{acetone}]$  can be made by considering that "free" **1** in acetone exists as **1**·acetone. The concentration of acetone is considered constant and has therefore not been taken into account in the expression of *K*. Attempts to fit the curve on the basis of a 1:2 complex formation gave rise to unstable refinement and were therefore unsuccessful.

**Synthesis of 1,2-Bis(chloromercurio)tetrafluorobenzene-Bis(dimethyl methylphosphonate) Adduct (3).** Compound **1** (62 mg, 0.1 mmol) was dissolved in 1 mL of hot DMMP (100 °C). When the solution was cooled, needlelike crystals of **3** spontaneously precipitated and were isolated dried over a paper towel (Kimwipes). Yield: 70% (60 mg). Mp: 103–105 °C. Anal. Calcd for C<sub>12</sub>H<sub>18</sub>Cl<sub>2</sub>F<sub>4</sub>Hg<sub>2</sub>P<sub>2</sub>O<sub>6</sub>: C, 16.59; H, 2.07. Found C, 16.62; H, 2.03. <sup>31</sup>P{<sup>1</sup>H} CP/MAS NMR: δ 35.6 (s, 1P), 37.5 (br, 1P). IR (KBr): 3595, 3002, 2957, 2853, 1615, 1590, 1477, 1417, 1311, 1285, 1234, 1186, 1082, 1043, 1002, 917, 824, 795, 762, 634, 501 cm<sup>-1</sup>.

**Single-Crystal X-ray Analysis.** X-ray data for **3** were collected on a Bruker SMART-CCD diffractometer using graphite-monochromated Mo Kα radiation (λ = 0.710 73 Å). A colorless plate of approximately 0.40 × 0.06 × 0.02 mm<sup>3</sup> was selected for analysis and mounted on a glass fiber using epoxy cement. The data were collected using 0.3° wide ω scans with a crystal-to-detector distance of 5.0 cm, yielding a complete (97.5%) sphere of 25 803 (5476 unique, *R*<sub>int</sub> = 0.0584) data (3.78 < 2θ < 56.68°). The data were corrected for absorption empirically using the SADABS routine (*T*<sub>max</sub> = 0.7661, *T*<sub>min</sub> = 0.0708). The remaining important crystallographic data are collected in Table 1. The structure was solved by direct methods, which successfully located most of the non-hydrogen atoms. Subsequent refinement on *F*<sup>2</sup> using the SHELXTL/PC package (version 5.1) allowed location of the remaining non-hydrogen atoms. One of the DMMP molecules was found to be positionally disordered over two orientations that were related by an approximate mirror plane passing through the phosphonate oxygen atom (O(21)) and one of the carbon atoms (C(21)). Refinement of the relative contributions of each orientation converged to approximately 50:50 and was held fixed at this value during the final refinement. During the final refinement, the two positionally ordered atoms (O(21), C(21)) and the phosphorus atoms were refined anisotropically while the remaining atoms in this fragment were refined isotropically. All non-hydrogen atoms in the rest of the structure were refined anisotropically, and the hydrogen atoms were included in calculated positions using a standard riding model. The refinement converged with residuals of *R*1 = 0.0324 and *wR*2 = 0.0614 for 258 parameters and 3866 data with *I* > 2σ(*I*). The largest residual electron density peak (1.66 e/Å<sup>3</sup>) was located near one of the Hg–C bonds, while the largest hole (−1.07 e/Å<sup>3</sup>) was found near the disordered phosphorus atom.

**Acknowledgment.** We thank the Department of Chemistry at Texas A&M University for making this work possible. Financial support from the State of Bavaria/Technische Universität München and the Deutscher Akademischer Austauschdienst (Promotionsstipendium, grant to M.T.) is gratefully acknowledged. The purchase of the X-ray diffractometer was made possible by a grant from the National Science Foundation (No. CHE-9115394); additional support for its purchase was provided by Georgetown University.

**Supporting Information Available:** Crystallographic files, in CIF format, for complex **3**. This material is available free of charge via the Internet at <http://pubs.acs.org>.

OM990987H

(23) Zamora, F.; Sabat, M.; Janik, M.; Siethoff, C.; Lippert, B. *J. Chem. Soc., Chem. Commun.* **1997**, 485–486.

(24) Perfluorinated aryl groups are electron poor, which decreases  $\pi$ - $\pi$  repulsions and favors parallel stacking: (a) Cozzi, F.; Ponzini, F.; Annunziata, R.; Cinquini, M.; Siegel, J. S. *Angew. Chem., Int. Ed. Engl.* **1995**, *34*, 1019–1020. (b) Hunter, C. A.; Lu, X.-J.; Kapteijn, G. M.; van Koten, G. *J. Chem. Soc., Faraday Trans.* **1995**, *91*, 2009–2015.

(25) Beese, L. S.; Steitz, T. A. *EMBO J.* **1991**, *10*, 25–33. Numerous other examples can be found in the following review: Straeter, N.; Lipscomb, W. N.; Klabunde, T.; Krebs, B. *Angew. Chem., Int. Ed. Engl.* **1996**, *35*, 2025–2055.

(26) Massey, A. G.; Al-Jabar, N. A. A.; Humphries, R. E.; Deacon, G. B. *J. Organomet. Chem.* **1986**, *316*, 25–39.

(27) Hynes, M. J. *J. Chem. Soc., Dalton Trans.* **1993**, 311–312.